

# Self-similar galaxy dynamics below the de Sitter scale of acceleration

Maurice H.P.M. van Putten<sup>1</sup>

<sup>1</sup>*Physics and Astronomy, Sejong University, 98 Gunja-Dong Gwangjin-gu, Seoul 143-747, Korea*

## ABSTRACT

Radial accelerations  $\alpha$  in galaxy dynamics are now observed over an extended range in redshift that includes model calculations on galactic distributions of cold dark matter (CDM) in  $\Lambda$ CDM. In a compilation of data of the *Spitzer* Photometry and Accurate Rotation Curves (SPARC) catalogue, the recent sample of Genzel et al.(2017) and the McMaster Unbiased Galaxy Simulations 2, we report on effective self-similarity in the variable  $\zeta = a_N/a_{dS}$ , given by the Newtonian acceleration  $a_N$  based on baryonic matter content over the de Sitter scale of acceleration  $a_{dS} = cH$ , where  $c$  is the velocity of light and  $H$  is the Hubble parameter. SPARC, MUG2 and theory satisfy  $a_N/\alpha \simeq 2.1\zeta^{\frac{1}{2}}$  ( $\zeta \ll 1$ ). At  $\zeta = 1$  in transition to Newtonian gravity ( $\zeta \gg 1$ ), however, there is a  $6\sigma$  gap between SPARC and MUGS2. This poses a novel challenge to CDM in  $\Lambda$ CDM against the apparent  $C^0$  galaxy dynamics observed in SPARC. We attribute the latter to reduced inertia below the de Sitter scale of acceleration ( $\zeta < 1$ ), based on a causality constraint imposed by the cosmological horizon  $\mathcal{H}$ .

**Key words:** galaxy dynamics: observations

## 1 INTRODUCTION

Advances in high resolution spectroscopy of galaxy rotation curves across a range of redshifts give a detailed view on radial accelerations over an extended range in radius  $r$  and redshift  $z$  up to about two (Famae & McGaugh 2012; Lelli et al. 2016; McGaugh et al. 2016; Genzel et al. 2017). In  $\Lambda$ CDM, these observations suggest a diminishing of cold dark matter content with  $z$ , as observed accelerations  $\alpha$  increasingly match the Newtonian acceleration

$$a_N = \frac{GM_b}{r^2} \quad (1)$$

by baryonic matter content  $M_b$  within  $r$ , where  $G$  is Newton’s constant. These results provide important benchmarks for galaxy models in  $\Lambda$ CDM from high resolution smoothed particle hydrodynamics simulations of galaxy formation. A recent comparison of the McMaster Unbiased Galaxy Simulations 2 (MUGS2) sample of galaxy models, for instance, suggests excellent agreement with the “missing mass” in galaxy rotation curves from the *Spitzer* Photometry and Accurate Rotation Curves (SPARC) (Keller & Wadsley 2017). Here, we revisit this claim focused on the transition regime of gravitational acceleration consistent with Newton’s theory based on baryonic matter and weak gravitation, marked by anomalous dynamics commonly attributed to dark matter or a modification of Newtonian gravitation (Famae & McGaugh 2012).

In a model-independent approach, redshift dependence

in galaxy dynamics shows evolution with background cosmology described by the Hubble parameter  $H = H(z)$ , carrying a de Sitter scale of acceleration

$$a_{dS} = cH, \quad (2)$$

where  $c$  is the velocity of light and  $H$  is the Hubble parameter (Fig. 1). For a galaxy such as the Milky Way,  $a_N = a_{dS}$  corresponds to a distance (van Putten 2016)

$$r_t = \sqrt{R_g R_H} = 4.6 \text{ kpc } M_{11}^{1/2}, \quad (3)$$

where  $R_H = c/H$  is the Hubble radius in a three-flat Friedmann-Robertson-Walker universe and  $R_g = GM/c^2$  is the gravitational radius of a galaxy of mass  $M = M_{11}10^{11}M_\odot$ . In quantum cosmology,  $a_{dS}$  represents the surface gravity of the cosmological horizon at Hubble radius  $R_H = c/H$  in de Sitter space (Gibbons & Hawking 1977). Based on dimensional analysis, this suggests evolution in galaxy dynamics in

$$\zeta = \frac{a_N}{a_{dS}}, \quad (4)$$

where  $\zeta = 1$  corresponds to a collusion of Rindler and cosmological horizon (van Putten 2017b).

We here consider data on galaxy dynamics as a function of  $\zeta$ , of galaxy rotation curves of observed galaxies and numerical galaxy models in  $\Lambda$ CDM side-by-side (§2). This compilation highlights *self-similar behavior* in galaxy dynamics in  $\zeta$  - by which data over different redshifts coalescence - and a transition across  $\zeta = 1$  to weak gravitation ( $\zeta < 1$ )

from normal, Newtonian gravitation ( $\zeta > 1$ ), where observed and modeled galaxy dynamics differ. These observations are interpreted in §3. This study is restricted to late-time cosmology with redshifts  $z$  up to about two, over which range the Hubble parameter varies by a factor up to about three (Fig. 1). In §4, we give our conclusions and outlook on future observations.

## 2 SELF-SIMILAR GALAXY DYNAMICS

Galaxy rotation data considered here are taken from SPARC (McGaugh et al. 2016; Lelli et al. 2016), MUGS2 (Keller & Wadsley 2017) and Genzel et al. (2017).

SPARC provides a sample of rotation curves observed from 175 nearby mostly late Hubble type galaxies observed by spectroscopy and photometry in  $\text{H}\alpha$ , covering a broad range in luminosity ( $10^{7-12} L_\odot$ ), radii (0.3–15 kpc), effective surface brightness ( $5 - 5000 L_\odot \text{pc}^{-2}$ ) and rotation velocities ( $20 - 300 \text{ km s}^{-2}$ ) consistent with a stellar mass-to-light ratio  $0.5 M_\odot / L_\odot$ .

MUGS2 provides a sample of 18 galaxy models with halo masses  $3.7 \times 10^{11} - 2.2 \times 10^{12} M_\odot$  and disk masses  $1.8 \times 10^{10} - 2.7 \times 10^{11} M_\odot$  in a  $\Lambda\text{CDM}$  cosmology from high resolution smoothed particle hydrodynamics simulations with radiative cooling, star-formation and feedback from supernovae (Wadsley et al. 2004; Volker 2005; Shen et al. 2010; Keller et al. 2014). Excluding galaxies that experience appreciable tidal interactions and limited to galaxies modeled by at least 100 star particles, it is extended to a total of 32 galaxies at  $z = 0$  (Keller & Wadsley 2017).

Genzel et al. (2017) provides a sample of six rotation curves of galaxies at intermediate redshifts  $z \in \{0.854, 1.5, 1.613, 2.196, 2.242, 2.383\}$  with respective baryonic masses  $M_{b,11} = \{1.7, 2.3, 1.0, 1.7, 1.7, 2.1\}$  and  $\Lambda\text{CDM}$  Hubble parameters  $H(z)/H_0 = \{1.599, 2.288, 2.425, 3.190, 3.253, 3.454\}$  featuring rotation velocities  $V_c = \{276, 310, 257, 301, 364, 299\} \text{ km/s}$  at radii  $R_{1/2} = \{7.3, 7.4, 4.9, 5.5, 3.3, 6\} \text{ kpc}$ . Following (9), their  $\zeta$  values cluster about  $\zeta = 1$  (van Putten 2017b),

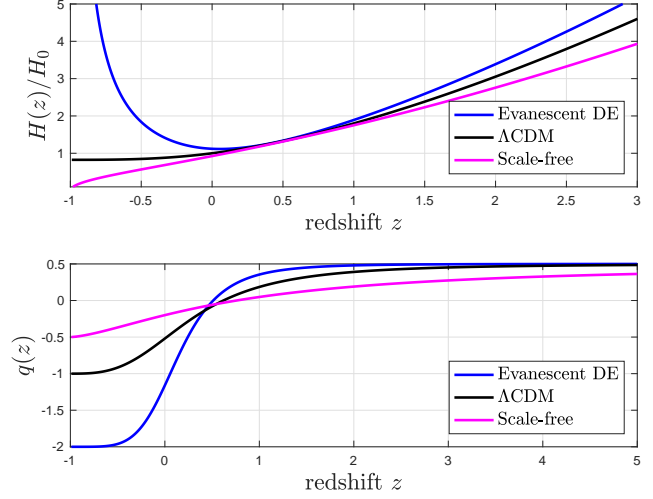
$$\zeta = \{0.2942, 0.3100, 0.3162, 0.3378, 0.4034, 0.8521\}. \quad (5)$$

Fig. 2 shows a compilation of MUGS2 rotation curve data plotted as a function of  $\zeta$ . Over  $0 \leq \zeta \leq 2$ ,  $H(z)$  varies by a factor of about three, implying variations of order unity in dimensional quantities such as  $r_t$ . For MUGS2, averaging of rotation curve data  $(\zeta, a_N/\alpha)_{z_k}$  over different redshifts leaves a dispersion much smaller than scatter in the data.

Fig. 3 shows a compilation of the three galaxy samples of SPARC, Genzel et al. (2017) and MUGS2 combined. While there is excellent agreement between SPARC and MUGS2 in the weak gravity limit  $\zeta \ll 1$ , there appears to be an appreciable gap about  $\zeta = 1$  in transition to the Newtonian limit  $\zeta \gg 1$ . As a function of  $\zeta$ , the relatively high redshift data from Genzel et al. (2017) agree within uncertainties with SPARC except for the outlier cZ 4006690.

Plotted as a function of  $\zeta$ , the aforementioned “missing mass” in galaxy rotation curves appears to be *self-similar* over an extended range of redshift, absorbed in normalization by  $a_{dS}$  giving a *reduction in independent variables by one*.

In the outskirts of galaxies, rotation curves satisfy



**Figure 1.** Evolution of the Hubble parameter  $H$  in cosmologies with different models of dark energy and the associated deceleration parameter  $q(z) = -1 + (1+z)H^{-1}(z)H'(z)$  as a function of redshift  $z$ . Next to  $\Lambda\text{CDM}$  are shown evolution by evanescent dark energy ( $\Lambda = \omega_0^2$  set by the eigenfrequency  $\omega_0^2$  of the cosmological horizon (van Putten 2017b)) and a scale-free cosmology (Maeder 2017; Jesus 2017). These models have similar evolution in the past ( $z > 0$ ), showing an increase in  $H$  by a factor of about two (three) at  $z = 1$  ( $z = 2$ ), while showing dramatically different behavior in the future ( $-1 < z < 0$ ).

Milgrom (1983)’s law,  $\alpha = \sqrt{a_0 a_N}$  with (van Putten 2017b)

$$a_0 = \frac{\omega_0}{2\pi}, \quad (6)$$

based on the fundamental frequency  $\omega_0 = \sqrt{1-q} a_{dS}$  of the Hubble horizon, where  $q = q(z)$ ,  $q(z) = -1 + (1+z)H^{-1}(z)H'(z)$  is the deceleration parameter. In the asymptotic regime  $\zeta \ll 1$ , therefore, we have

$$\frac{a_N}{\alpha} = (2\pi)^{\frac{1}{2}} (1-q)^{-\frac{1}{4}} \zeta^{1/2} \simeq 2.1 \zeta^{\frac{1}{2}}, \quad (7)$$

where the right hand side refers to  $z \simeq 0$ . Deviations from self-similarity by  $\pm 20\%$  in  $(1-q)^{\frac{1}{4}}$  as  $q$  varies over  $-1 < q < 0.5$  in late-time cosmology are too small to be resolved in the present data.

## 3 A $6\sigma$ GAP AT $\zeta = 1$

In transition from Newtonian gravity (1) ( $\zeta \gg 1$ ) to weak gravity ( $\zeta \ll 1$ ), Fig. 3 shows an onset to the latter which is smooth in MUGS2 in contrast to what appears to be  $C^0$  galaxy dynamics - continuous with discontinuous derivatives - in SPARC (van Putten 2017b). (Uncertainties in the data do not resolve whether the transition is truly  $C^0$  or nearly so.) Smoothness in MUGS2 is expected and inherent to  $N$ -body simulations by diffusion due to small angle gravitational scattering and gas dynamics. The noticeable gap between MUGS2 and SPARC at  $\zeta = 1$  hereby might be characteristic for galaxy models in  $\Lambda\text{CDM}$ , not limited to MUGS2.

It is perhaps paradoxical, that  $\zeta$  is a similarity variable familiar from the theory of linear diffusion, yet the apparent  $C^0$  onset to weak gravity in SPARC runs counter to the

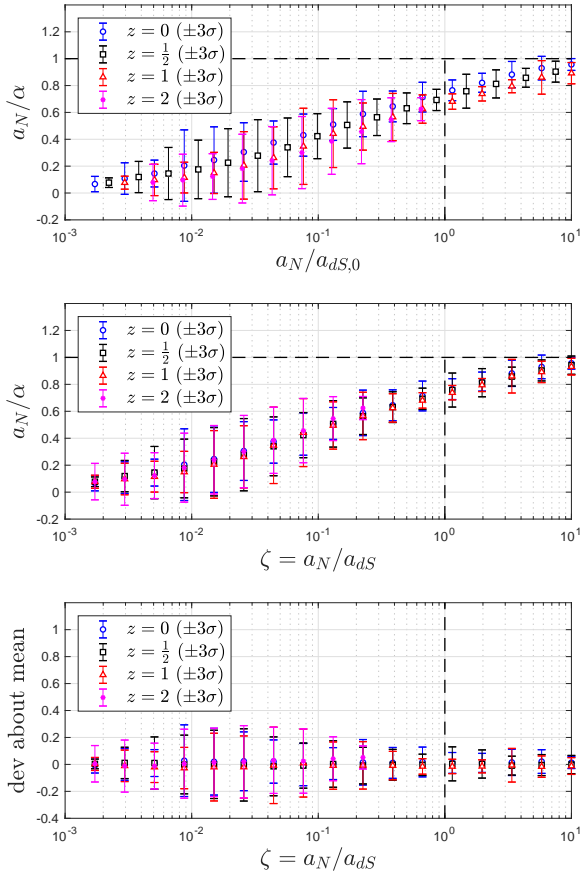


**Figure 2.** Compilation of radial accelerations in MUGS2 data (Keller & Wadsley 2017) in  $\Lambda$ CDM numerical galaxy models plotting rotation curve data as  $a_N/\alpha$  versus  $a_N/a_{dS,0}$  (top panel) and versus the similarity variable  $\zeta = a_N/a_{dS}$  (middle panel), covering weak gravity ( $a_N/a_{dS} < 1$ ) and Newtonian gravity  $a_N/a_{dS} \geq 1$  of baryonic matter content (black dashed). The results show remarkable self-similarity in  $\zeta$ , in galaxy evolution tracing background cosmology with Hubble parameter increasing by a factor of a few over  $0 \leq z \leq 2$ . For  $z = 2$ , data are limited to  $\zeta \leq 0.2254$ . For each  $z$ , deviations from the mean of rotation curve data (over  $z = 0, \frac{1}{2}, 1$ ) are much smaller than statistical errors in this average (bottom panel).

same. We attribute this result to a break in Newton’s second law - assuming a constant inertia at arbitrarily small accelerations - on a cosmological background with finite Hubble radius  $R_H$ , equivalently attributed to thermodynamic properties of the associated cosmological horizon  $\mathcal{H}$ .

According to the equivalence principle of general relativity, inertia can be identified with inertial mass-energy (van Putten 2017b)

$$U = mc^2 \quad (8)$$

given by the gravitational binding energy in the gravitational field over the distance

$$\xi = \frac{c^2}{\alpha} \quad (9)$$

to the Rindler horizon  $h$  at a given acceleration  $\alpha$ . Here,  $U$  obtains by integrating the inertial force  $F = m\alpha$  over a distance  $\xi$ .

According to quantum field theory, the vacuum seen

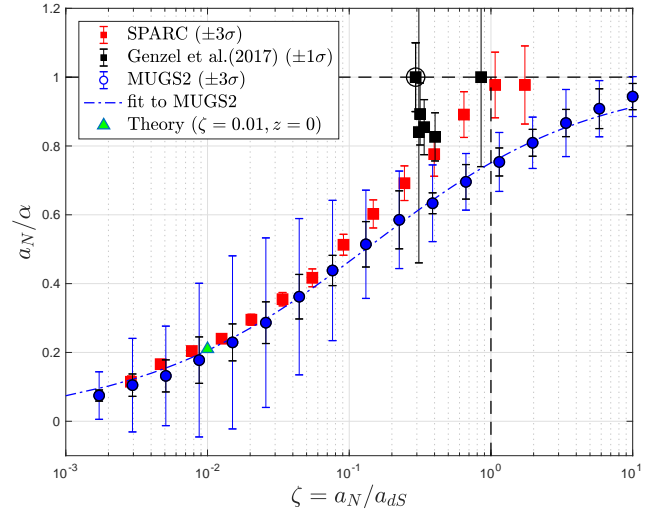


**Figure 3.** Radial accelerations in spiral galaxies from SPARC (red), Genzel et al. (2017) (black) and MUGS2 (blue:  $a_N/\alpha$  versus  $\zeta = a_N/a_{dS}$  covering weak gravity ( $a_N/a_{dS} < 1$ ) and Newtonian gravity  $a_N/a_{dS} \geq 1$  of baryonic matter content (black dashed). Error bars are  $3\sigma$  for data of SPARC and MUGS2 (uncertainties from scatter (blue) and averaging over redshift (black)) and  $1\sigma$  for (Genzel et al. 2017). SPARC covers  $z = 0$ , MUGS2  $z_k = 0, \frac{1}{2}, 1$  and  $z = 2$  ( $\zeta \leq 0.2254$ ), and Genzel et al. galaxies have  $\zeta$  clustered about  $\zeta = 1$ . For the latter, highlighted is the galaxy cZ 4006690 (black circle), which may have systematic errors in the observed strong asymmetry of its rotation curve. Observations show remarkable self-similarity in  $\zeta$ , in galaxy evolution tracing background cosmology over redshifts up to a few. SPARC, MUGS2 and theory (Eq. 6) agree asymptotically  $\zeta \ll 1$ . At  $\zeta = 1$ , SPARC appears to show  $C^0$  galaxy dynamics (continuous with discontinuous derivative) (van Putten 2017a,b), while MUGS2 provides a smooth interpolation with a  $6\sigma$  discrepancy at  $\zeta = 1$ .

by a Rindler observer is described by a finite temperature diffusion constant (reviewed by Son & Starinets 2007)

$$D = \frac{\hbar c^2}{2\pi k_B T} \quad (10)$$

where  $\hbar$  is Planck’s constant and  $k_B$  is the Boltzmann constant. With  $D = \xi c$ , (10) is the thermodynamic interpretation of Rindler’s relation (9) at the Unruh temperature  $T = T_U$  (Unruh 1976),

$$k_B T_U = \frac{\hbar \alpha}{2\pi c}. \quad (11)$$

Identifying  $T_U$  with the temperature of  $h$ ,  $U$  derives from the entanglement entropy  $I_1 = 2\pi\Delta\varphi_C$ , where  $\Delta\varphi_C$  is the distance  $\xi$  expressed in Compton phase (van Putten 2015), giving

$$U = \int_0^\xi T_U dI_1, \quad (12)$$

In (12),  $h$  is an apparent horizon surface. Apparent horizon surfaces are familiar concept in numerical relativity signaling black hole formation (Penrose 1965; Brewin 1988; Cook 2000; York 1989; Wald & Iyer 1991; Cook & Abrahams 1992; Thornburg 2007). In a three-flat Friedmann-Robertson-Walker universe, the cosmological horizon  $\mathcal{H}$  provides an apparent horizon in the background,

whose Hubble radius  $R_H$  puts a bound on  $\xi$ . As  $h$  formally drops beyond  $\mathcal{H}$  ( $\xi > R_H$ ),  $U$  in (8) drops below its Newtonian value  $m = m_0$ , since integration over the gravitational field is cut-off at  $R_H$  by  $\mathcal{H}$  as a causal boundary on  $D$  in (10). At a given  $a_N$ , the observed acceleration

$$\alpha = \left(\frac{m_0}{m}\right) a_N \quad (13)$$

experiences a  $C^0$  transition across  $\zeta = 1$  (van Putten 2017a,b). The apparent  $C^0$  galaxy dynamics in the SPARC data can hereby be attributed to causality imposed on inertial mass-energy by  $\mathcal{H}$ , leading to a  $6\sigma$  gap at  $\zeta = 1$  between it and MUGS2.

#### 4 CONCLUSIONS

An effective self-similarity  $\zeta$  in galaxy dynamics enables a comprehensive confrontation between galaxy rotation curves from observations and simulations over an extended range of redshifts, here shown in Fig. 3 for SPARC, MUGS2 and Genzel et al. galaxies covering redshifts up to about two. In weak gravity ( $\zeta \ll 1$ ), SPARC, MUGS2 and theory agree. At  $\zeta = 1$ , however, there is a  $6\sigma$  gap between SPARC and MUGS2, where the first appears to show  $C^0$  galaxy dynamics while the second gives a smooth transition between  $\zeta \ll 1$  and the Newtonian regime  $\zeta \gg 1$ . In Fig. 3, the latter is emphasized by a simple fitting function

$$\frac{a_N}{\alpha} = \left(\frac{1}{2} + \sqrt{\frac{1}{4} + \frac{1}{x} + \frac{1}{\sqrt{x}}}\right)^{-1} \quad (14)$$

with  $x = 4\pi\zeta$ . This gap appears to have eluded the previous analysis of Keller & Wadsley (2017).

The low apparent dark matter content in Genzel et al. (2017) arises from clustering of  $\zeta$  close to the transition point  $\zeta = 1$ , that agrees with SPARC but deviates from MUGS2. Conversely, there is no apparent low dark matter content in high redshift galaxies of MUGS2.

The SPARC-MUGS2 gap is expected to be generic for CDM galaxy models in  $\Lambda$ CDM, resulting from smoothness inherent to diffusion by small angle gravitational scattering. At  $6\sigma$ , this discrepancy appears to be fundamental to the nature of CDM, unless perhaps the mass of the putative dark matter particle is anomalously small. The apparent  $C^0$  galaxy dynamics in SPARC, however, points to a departure of Newton's second law as inertia drops at accelerations below  $a_{dS}$ , when inertial mass-energy  $U$  reduces to gravitational binding energy to the cosmological horizon  $\mathcal{H}$ .

While a reduced inertia obviates the need for CDM in galaxies, a cosmological distribution of CDM is still required in light of the three-flat condition  $\Omega_M + \Omega_\Lambda = 1$  on the dimensionless densities of dark matter ( $\Omega_M$ ) and dark energy ( $\Omega_\Lambda$ ). The Compton wave length of the putative dark matter particle, greater than the scale of galaxies, may reach the scale of galaxy clusters.

In light of the above, we anticipate that the apparent self-similarity and  $C^0$  galaxy dynamics shown in Figs. 2-3 extends to elliptical galaxies, which may be obtained through future studies given the very large samples of elliptical galaxies available from, e.g., the *Sloan Digital Sky Survey* (Abolfati et al. 2018).

*Acknowledgements.* The author thanks B. Keller for

kindly providing the MUGS2 data shown in Fig. 2, the anonymous reviewer for detailed comments which greatly improved this manuscript, and K.-H. Chae for stimulating discussions on interpolation functions.

This research is supported in part by the National Research Foundation of Korea (No. 2015R1D1A1A01059793, 2016R1A5A1013277 and 2018044640)

#### REFERENCES

- Abolfati, B., Aguado, D.S., Aguilar, G., et al., 2018, *ApJ Suppl.*, 235, 42
- Planck Collaboration, Ade, P. A. R., Aghanim, N., et al. 2016, *A&A*, 594, A13
- Anderson, R.I., & Riess, A.G., 2017, arXiv: 1712.01065v1
- Brewin, L., 1988, *Phys. Rev. D*, 38, 3020;
- Cook, G.B., & Abrahams, A.M., 1992, *Phys. Rev. D*, 46, 702
- Cook, G. B. 2000, *LRR*, 3, 5
- Famae, G., & McGaugh, S.S., 2012, *Liv. Rev. Rel.*, 1
- Freedman, W.L., 2017, *Nat. Astron.*, 1, 0121
- Genzel, R., Förster Schreiber, N. M., Übler, H., et al. 2017, *Natur*, 543, 397
- Gibbons, G. W., & Hawking, S. W. 1977, *PhRvD*, 15, 2738
- Hawking, S., 1975, *Commun. Math. Phys.* 43, 199
- Jesus, J.F., 2017, arXiv:1712.00697
- Keller, B.W., Wadsley, J., Benincasa, S.M., & Couchmanm H.M.P., 2014, *MNRAS*, 442, 3013
- Keller, B.W., & Wadsley, J.W., 2017, *ApJ*, 835, L17
- Lelli, F., McGaugh, S. S., & Schombert, J. M. 2016, *AJ*, 152, 157
- McGaugh, S. S., Lelli, S., & Schombert, J. M. 2016, *PhRvL*, 117, 201101
- Maeder, A., 2017, *ApJ*, 849, 194
- Milgrom, M, 1983, *ApJ*, 270, 365
- Penrose, R., 1965, *Phys. Rev. Lett.*, 14, 57
- Shen, S., Wadsley, J., & Stinson, G., 2010, *MNRAS*, 407, 1581
- Son, D.T., & Starinets, A.O., 2007, *Annu. Rev. Nucl. Part. Sci.*, 57, 95
- Thornburg, J., 2007, *Liv. Rev. Rel.*, 10, 7
- Unruh, W. G. 1976, *PhRvD*, 14, 870
- van Putten, M.H.P.M., 2015, 24, 1550024
- van Putten, M.H.P.M., 2016, 824, 43
- van Putten, M.H.P.M., 2017, *ApJ*, 837, 22
- van Putten, M.H.P.M., 2017, *ApJ*, 848, 28
- Volker, S., 2005, *MNRAS*, 364, 1105
- Wadsley, J.W., Stadel, J., & Quinn, T., 2004, *NewA*, 9, 137
- Booth, I., 2005, *Can. J. Phys.*, 83, 1073
- Hawking, S.W., & Ellis, G.F.R., 1975, *The large scale structure of space-time* (Cambridge University Press)
- Wald, R.M., & Iyer, V., 1991, *Phys. Rev. D*, 44, R3719
- York, J.W., 1989, in *Frontiers in Numerical Relativity*, ed. C.R. Evans, L.S. Finn & D.W. Hobill (Cambridge University Press)